УДК 53.088:62 – 754.2 (045)

V. Apostolyuk, Ph.D. in Engineering,
(National Aviation University, Ukraine)

CORIOLIS VIBRATORY GYROSCOPES IN CONTROL SYSTEMS

This paper describes new method of Coriolis vibratory gyroscope dynamics analysis by means of complex amplitude-phase variables, introduces corresponding system transfer functions, and studies applicability of simplified transfer functions for the broader range of compatible devices.

In the most generalized form, motion equations of the sensitive element of Coriolis vibratory gyroscopes (CVG) could be represented in the following form [1]:

$$\begin{cases} \ddot{x}_1 + 2\zeta_1 k_1 \dot{x}_1 + (k_1^2 - d_1\Omega^2)x_1 + g_1\Omega\dot{x}_2 + d_3\dot{\Omega}x_2 = q_1(t), \\ \ddot{x}_2 + 2\zeta_2 k_2 \dot{x}_2 + (k_2^2 - d_2\Omega^2)x_2 - g_2\Omega\dot{x}_1 - \dot{\Omega}x_1 = q_2(t). \end{cases} \quad (1)$$

Here x_1 and x_2 are the generalized coordinates that describe primary (excited) and secondary (sensed) motions of the sensitive element respectively, k_1 and k_2 are the corresponding natural frequencies, ζ_1 and ζ_2 are the dimensionless relative damping coefficients, Ω is the measured angular rate, which is orthogonal to the axes of primary and secondary motions, q_1 and q_2 are the generalized accelerations due to the external forces acting on the sensitive element. The remaining dimensionless coefficients are different for the sensitive elements exploiting either translational or rotational motion. For the translational sensitive element they are $d_1 = d_2 = 1$, $d_3 = m_2/(m_1 + m_2)$, $g_1 = 2m_2/(m_1 + m_2)$, $g_2 = 2$, where were m_1 and m_2 are the masses of the outer frame and the internal massive element. In case of the rotational motion of the sensitive element, these coefficients are the functions of different moments of inertia (for greater details see [1]).

In order to make the equations (1) suitable for the demodulated signals analysis we must make the following assumptions: angular rate is small comparing to the primary and secondary natural frequencies so that

$$k_1^2 >> d_1\Omega^2,\ k_2^2 >> d_2\Omega^2, \quad (2)$$

and rotational and Coriolis accelerations acting along primary oscillation axis are negligible in comparison to the accelerations from driving forces

$$g_1\Omega\dot{x}_2 + d_3\dot{\Omega}x_2 << q_1(t). \quad (3)$$

Taking into considerations assumptions (2) and (3), motions equations (1) could be simplified to the following form:

$$\begin{cases} \ddot{x}_1 + 2\zeta_1 k_1 \dot{x}_1 + k_1^2 x_1 = q_1(t), \\ \ddot{x}_2 + 2\zeta_2 k_2 \dot{x}_2 + k_2^2 x_2 = g_2\Omega\dot{x}_1 + \dot{\Omega}x_1. \end{cases} \quad (4)$$

Here we also assumed that no external driving forces are affecting the secondary oscillations, which means that $q_2(t) = 0$. System of equations (4) is now perfectly suitable for further transformations towards the desired representation in terms of the unknown angular rate.

As has been shown in [5], by means of a proper chosen phase shift of the excitation voltage applied to the sensitive element, the excitation force could be shaped to the perfect harmonic form. Using exponential representation of complex numbers, such a driving force $q_1(t)$ could be represented as

$$q_1(t) = q_{10}\sin(\omega t) = \mathrm{Im}\{q_{10}e^{j\omega t}\}. \quad (5)$$

Here ω is the excitation frequency given in radians per second, q_{10} is the constant excitation acceleration amplitude. Non-homogeneous solutions of the motion equations (1) or (4) for primary and secondary oscillations are searched in a similar form

$$\begin{aligned} x_1(t) &= \mathrm{Im}\{A_1(t)e^{j\omega t}\}, \quad A_1(t) = A_{10}(t)e^{j\varphi_{10}(t)}, \\ x_2(t) &= \mathrm{Im}\{A_2(t)e^{j\omega t}\}, \quad A_2(t) = A_{20}(t)e^{j\varphi_{20}(t)}, \end{aligned} \tag{6}$$

where A_{10} and A_{20} are the primary and secondary oscillation amplitudes, φ_{10} and φ_{20} are the corresponding phase shifts relatively to the excitation force. Although these quantities are real (non-imaginary), they are combined in complex amplitude-phase variables A_1 and A_2.

Substituting expressions (5) and (6) into equations (4) results in the following motions equations in terms of the complex amplitude-phase variables rather than real generalized coordinates:

$$\begin{cases} \ddot{A}_1 + 2(\zeta_1 k_1 + j\omega)\dot{A}_1 + (k_1^2 - \omega^2 + 2j\omega k_1\zeta_1)A_1 = q_{10}, \\ \ddot{A}_2 + 2(\zeta_2 k_2 + j\omega)\dot{A}_2 + (k_2^2 - \omega^2 + 2j\omega k_2\zeta_2)A_2 = (j\omega g_2\Omega + \dot{\Omega})A_1 + g_2\dot{A}_1\Omega. \end{cases} \tag{7}$$

Equations (7) describe variations of the amplitude and phase of the primary and secondary equations in time with respect to the unknown non-constant angular rate $\Omega(t)$. This allows conducting analysis of the Coriolis vibratory gyroscope dynamics without constraining the angular rate to be constant or slowly varying.

Analysing system (7), one can see that the first equation can be solved separately from the second one. After homogeneous solutions of the first equation faded out, only non-homogenous solution remains. In this case, amplitude of the primary oscillations is

$$A_1 = \frac{q_{10}}{k_1^2 - \omega^2 + 2jk_1\zeta_1\omega}, \tag{8}$$

and it is constant in time, yielding $\ddot{A}_1 = \dot{A}_1 = 0$. Indeed, most of the time measurements of the angular rate are performed when primary oscillations have already settled. As a result, only equation for the secondary oscillations remains, in which the complex primary amplitude A_1 is just a constant parameter given by (8):

$$\ddot{A}_2 + 2(\zeta_2 k_2 + j\omega)\dot{A}_2 + (k_2^2 - \omega^2 + 2j\omega k_2\zeta_2)A_2 = (j\omega g_2\Omega + \dot{\Omega})A_1. \tag{9}$$

Equation (7) now describes amplitude-phase of the secondary oscillations with respect to the settled primary oscillations.

Having CVG sensitive element motion equation in the form (9), allows analysis of its transient processes in amplitudes and phases with respect to arbitrary angular rates applied to the system. Application of the Laplace transformation to the equations (7) with respect to zero initial conditions for all time-dependent variables results in the following expressions:

$$[(s + j\omega)^2 + 2\zeta_2 k_2(s + j\omega) + k_2^2]A_2(s) = A_1[s + jg_2\omega]\Omega(s). \tag{10}$$

Solution of the algebraic equation (10) for the secondary amplitude-phase Laplace transform is

$$A_2(s) = \frac{A_1(s + jg_2\omega)}{(s + j\omega)^2 + 2\zeta_2 k_2(s + j\omega) + k_2^2}\Omega(s). \tag{11}$$

Considering the angular rate as an input, the system transfer function for the secondary amplitude-phase is

$$\begin{aligned} W_2(s) = \frac{A_2(s)}{\Omega(s)} &= \frac{A_1(s + jg_2\omega)}{(s + j\omega)^2 + 2\zeta_2 k_2(s + j\omega) + k_2^2} = \\ &= \frac{q_{10}(s + jg_2\omega)}{[(s + j\omega)^2 + 2\zeta_2 k_2(s + j\omega) + k_2^2][k_1^2 - \omega^2 + 2j\omega k_1\zeta_1]}. \end{aligned} \tag{12}$$

One should note that transfer function (12) has complex coefficients, which results in the complex system outputs as well. Although it is somewhat unusual, it still enables us to analyse CVG dynamics and transient processes due to the angular rate in an open-loop dynamic system.

One can see that actual amplitude of the secondary oscillations is mainly defined by the low frequency oscillations, while effect from the high frequency components can be neglected, since it will be removed during demodulation process. In other words, predominant behaviour is a slow variation of the amplitude and phase. Neglecting the second order derivative in the equation (9) yields

$$2(\zeta_2 k_2 + j\omega)\dot{A}_2 + (k_2^2 - \omega^2 + 2j\omega k_2\zeta_2)A_2 = (j\omega g_2\Omega + \dot{\Omega})A_1, \tag{13}$$

and the corresponding angular rate transfer function becomes

$$W_2(s) = \frac{q_{10}(s + jg_2\omega)}{[2\zeta_2 k_2 s + k_2^2 - \omega^2 + j2\omega(\zeta_2 k_2 + s)][k_1^2 - \omega^2 + 2j\omega k_1\zeta_1]}. \tag{14}$$

While simulating dynamics of CVG based on the complex amplitude-phase transfer functions (12) or (14) one could have problems dealing with complex coefficients of these transfer functions. One way to avoid this problem is to consider real and imaginary parts of complex amplitude as separate signals, which are then combined together to produce real amplitude and phase. In order to obtain transfer functions for such signals let us represent primary and secondary amplitudes as:

$$A_1 = A_{1R} + jA_{1I},\ A_2 = A_{2R} + jA_{2I}. \tag{15}$$

Primary oscillations components can be easily found by means of substituting expressions (15) into (8) thus yielding

$$A_{1R} = \frac{q_{10}(k_1^2 - \omega^2)}{(k_1^2 - \omega^2)^2 + 4k_1^2\zeta_1^2\omega^2},\ \ A_{1I} = -\frac{2q_{10}j\omega k_1\zeta_1}{(k_1^2 - \omega^2)^2 + 4k_1^2\zeta_1^2\omega^2}. \tag{16}$$

At the same time, substituting expressions (23) into the motion equation (9), and applying Laplace transformation gives

$$\begin{cases}(k_2^2 - \omega^2 + 2k_2\zeta_2 s + s^2)A_{2R} - 2\omega(k_2\zeta_2 + s)A_{2I} = (A_{1R}s - A_{1I}g_2\omega)\Omega,\\ (k_2^2 - \omega^2 + 2k_2\zeta_2 s + s^2)A_{2I} + 2\omega(k_2\zeta_2 + s)A_{2R} = (A_{1I}s + A_{1R}g_2\omega)\Omega.\end{cases} \tag{17}$$

Resolving algebraic system (17) with respect to unknown real and imaginary parts of the secondary complex amplitude yields

$$A_{2R} = \frac{A_{1R}M_{RR}(s) + A_{1I}M_{RI}(s)}{P(s)}\Omega,\ \ A_{2I} = \frac{A_{1R}M_{IR}(s) + A_{1I}M_{II}(s)}{P(s)}\Omega. \tag{18}$$

Here the numerator polynomials from the real and imaginary parts of primary amplitudes are given by the following expressions:

$$\begin{aligned}M_{RR}(s) &= s(k_2^2 + 2k_2\zeta_2 s + s^2) - \omega^2(s - 2g_2(s + k_2\zeta_2))\\ M_{RI}(s) &= \omega[2s(s + k_2\zeta_2) - g_2(k_2^2 - \omega^2 + 2k_2\zeta_2 s + s^2)],\\ M_{II}(s) &= 2\omega^2 g_2(s + k_2\zeta_2) + s(k_2^2 - \omega^2 + 2k_2\zeta_2 s + s^2)],\\ M_{IR}(s) &= \omega[g_2(k_2^2 - \omega^2 + 2k_2\zeta_2 s + s^2) - 2s(s + k_2\zeta_2)].\\ P(s) &= 4(s + k_2\zeta_2)^2\omega^2 + (k_2^2 - \omega^2 + 2k_2\zeta_2 s + s^2)^2\end{aligned} \tag{19}$$

One should note that if primary oscillations are excited at the primary natural frequency ($\omega = k_1$), then

$$A_{1I} = -\frac{q_{10}}{2k_1^2\zeta_1},\ \ A_{1R} = 0, \tag{20}$$

and two out of the four transfer functions (19) become unnecessary.

Finally, there is quite an important case, when complex transfer functions transform to the simple real one. Assuming equal primary and secondary natural frequencies ($k_1 = k_2 = k$), equal damping ratios ($\zeta_1 = \zeta_2 = \zeta$), resonance excitation, and constant angular rate, one can easily obtain

$$A_{20}(s) = \sqrt{A_{2R}^2 + A_{2I}^2} = \frac{q_{10}g_2}{4k^2\zeta(s + k\zeta)}. \tag{21}$$

Although this case appears to be very specific, it still approximates transient process of a “tuned” CVG with accuracy suitable for most of the applications. Integral error of the transient process representation for the “un-tuned” sensitive elements as a function of the natural frequency ratio ($\delta k = k_2 / k_1$) and relative damping ratio ($\delta\zeta = \zeta_2 / \zeta_1$) is shown in the figure 1.

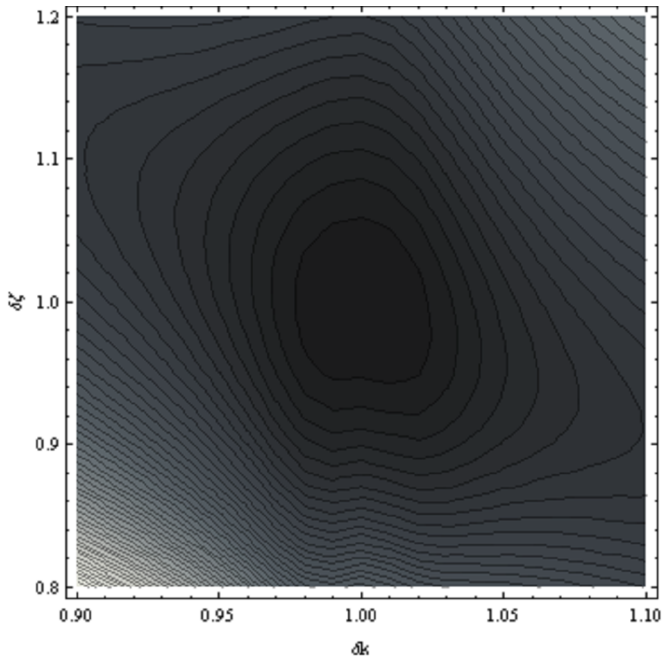

Fig. 1. Integral error of transient process representation

In this figure darker colours correspond to the zero error of the transient process representation. Here the central dark spot corresponds to the perfectly tuned device. One can see, that wide range of sensitive elements with varying ratio of the natural frequencies and ratio of relative damping still could be represented by the transfer function (21) with acceptably low integral error.

Conclusions

Presented above analysis of CVG dynamics using amplitude-phase complex variables resulted in obtaining system transfer functions, where measured angular rate became an input rather than a parameter. This makes possible to analyse amplitude and phase responses of CVG, its transient processes in already demodulated signals, optimise transient process characteristics. Excellent performance of the obtained simplified transfer functions has been demonstrated using numerical analysis of the integral error analysis.

References

[1] Apostolyuk V. A., Logeeswaran V.J., Tay F.E.H. Efficient design of micromechanical gyroscopes // Journal of Micromechanics and Microengineering, Vol. 12, 2002, pp. 948-954.

[2] Apostolyuk V. A. Theory and Design of Micromechanical Vibratory Gyroscopes // MEMS/NEMS Handbook (Ed: Cornelius T. Leondes), Springer, 2006, Vol.1, Chapter 6, pp. 173-195.

[3] Apostolyuk V.A. Dynamic Errors of Coriolis Vibratory Gyroscopes // Mechanics of Gyroscopic Systems, no. 19, 2008, pp. 230-239.